CrossMark

Post deposition annealing: a route to bandgap tailoring of ZnSe thin films

Nawazish A. Khan[1] · Abida Saleem[2] · Anees-ur-Rahman Satti[1] · M. Imran[1] · A. A. Khurram[3]

Abstract The ZnSe semiconductor thin films thermally evaporated on a glass substrate and an ITO substrate are studied and compared for their optical properties. Surprisingly, two different values of band gaps 2.49 and 2.91 eV in ZnSe thin films are observed, respectively deposited on glass substrate and ITO substrate. Similarly, the ZnSe films on ITO substrate has shown a hexagonal crystal structure with higher crystallinity as compared to that of ZnSe on glass. The ZnSe thin films deposited on glass substrate are also annealed at 350, 400, 450 and 500 °C under vacuum conditions, which has been resulted in improvement in crystallinity and increase in band gap energy from 2.45 to 2.54 eV. The ZnSe thin film deposited on ITO coated glass were annealed in vacuum and air at 450 °C. The air annealing has been resulted in a large increase in energy bandgap from 2.9 to 3.21 eV. It is also observed from these studies that the electrical conductivity of the films annealed in vacuum is higher than those of the annealed in air.

1 Introduction

Zinc Selenided (ZnSe) with a direct band-gap of 2.7 eV is found to be a very promising material for optoelectronic and heterojunction solar cells applications. It is used in many applications such as light-emitting diodes [1], photodiodes [2, 3], protective and antireflection coatings for infrared-operating electrochronic thermal-control surfaces [4], and dielectric mirrors [5]. Since most electronic devices are produced in the form of thin films for such applications, therefore, the material preparation and crystalline quality play a vital role which largely depend on the ambient pressure, lattice match with the substrate and post deposition treatments [6]. The photoelectronic and other properties of II–VI compound thin films are highly structure sensitive. The structural parameters like crystalline size, crystal phase, lattice constant, average stress and strain, etc. are strongly dependent on the deposition parameters and annealing temperature. A broad variety of techniques has been used for the deposition of ZnSe films, such as metal organic chemical vapour deposition (MOCVD) [7], molecular beam epitaxy (MBE) [8], metal organic vapour phase epitaxy (MOVPE) [8], RF magnetron sputtering [9], and vacuum evaporation [10]. Vacuum evaporation technique is relatively simple, inexpensive and in particular useful for large-area depositions. In this article we discussed the structural, optical and electrical properties and composition of ZnSe thin films deposited by using vacuum evaporation technique. The structure and energy bandgap of thermally evaporated ZnSe thin films is likely to be governed by the rate of deposition, substrate temperature, composition and annealing temperature. The post deposition annealing of ZnSe thin films is commonly used to achieve the crystalline phase of that material. However, the environment provided for the annealing can effect the

✉ A. A. Khurram
khuram_qau@yahoo.com

1 Materials Science Laboratory, Department of Physics, Quaid-i-Azam University, Islamabad 45320, Pakistan

2 Quaid-i-Azam University, Islamabad Campus, NCP Complex, Shadhara Valley Road, Islamabad, Pakistan

3 Industrial Technology Development, Quaid-i-Azam University, Islamabad Campus, NCP Complex, Shadhara Valley Road, Islamabad, Pakistan

optical bandgap of the semiconductor films due to the intercalation of oxygen. Another effect of annealing is the elimination of crystal imperfections resulting in the desired bandgap of the semiconductor. In most of the literature, the narrowing or widening of the bandgap of polycrystalline ZnSe thin films has been attributed to the increase or decrease of crystallite size [11–17]. However, in the present study, we have designed post-deposition annealing experiments at different temperatures in different ambient to study the effect of effect oxygen intercalation or reduction on the bandgap of ZnSe thin films. In the literature the effect of the use of a practical substrate such as ITO coated glass on the optical and structural properties is missing. We have also compared the structural and optical properties of ZnSe thin films deposited on glass and ITO coated glass substrates.

2 Experimental

The 99.999 % pure ZnSe trace metal basis powder was purchased from Sigma Aldrich. Thin films of ZnSe were deposited on glass and ITO coated glass substrates by thermal evaporation in Edward coating unit. The ZnSe powder was placed in a tantalum boat and the films have been deposited on borosilicate glass substrate under 10^{-4} mbar vacuum. The source to substrate distance was kept at 12 cm during deposition. We did not apply special heating for the substrate during deposition. Since we have used borosilicate glass substrates in both cases, which have higher anneal point and softening point, therefore, the selected deposition and annealing temperatures do not affect the glass itself. The post deposition annealing of the films was carried out for 10 min for each sample in the temperature range 350–500 °C under rough vacuum conditions. The temperature during annealing was slowly increased to desired set value and after annealing the samples have been cooled slowly to room temperature. After deposition, the films were characterized by X-ray diffraction (XRD), Rutherford Backscattering Spectrometry (RBS), UV visible spectroscopy and IV measurements to study their structure, composition, optical and electrical properties, respectively. Structural Studies were carried out by using a Bruker's X-ray diffractometer with CuK$_\alpha$ radiations (D8 FOCUS, $\lambda = 1.54056$). The 2θ scan was taken between 20° and 80° with a speed of 2°/min. RBS was used to find the composition and thickness of the films; in our work we used a normally incident 2.084 MeV He^{++} beam from a 5MV particle accelerator under high vacuum (10^{-6} torr). The detector resolution was 20 KeV. The RBS analysis was performed by using XRUMP and SIMNRA simulation softwares [18]. The DC electrical conductivity measurement was carried out by using four probe method.

The transmission spectra of ZnSe thin films on glass and ITO/glass substrates were taken in the wavelength range from 300 to 1200 nm by a optical spectrophotometer.

3 Results and discussion

The XRD of ZnSe thin film on glass substrate is shown in Fig. 1. It can be seen that the as prepared thin film is amorphous in nature. However, the post deposition annealing has improved the crystallinity of the film, which has been improved with the increase of annealing temperature. From the JCPD card number 892940 it is verified that ZnSe thin films have a zinc blend structure with a preferred orientation along (111) plane shown by a peak at $2\theta = 27.11°$, peak was shifted toward higher 2θ value after annealing. The analysis of XRD spectra shows that the lattice constant was decreased while the crystallite size has been increased with the increase of annealing temperature. The crystallite size, dislocation density and lattice strain were calculated from the XRD data by using the following formulas [19, 20].

$$D = \frac{0.94\lambda}{B\cos\theta}, \quad \varepsilon = \frac{B\cos\theta}{4}, \quad \delta = \frac{15\in}{aD}.$$

The RBS spectra taken to measure composition and thickness of ZnSe/glass films are shown in the Fig. 2. The intensity of the peaks is used to measure the concentration of the constituents. The RBS analysis of thin films are also used to study interface properties of thin film and substrate material. The RBS spectrum in 250–1000 channel range is due to the glass substrate. The high energy edge as shown in the inset of the figure belongs to Zn whereas, the next lower energy edge corresponds to Se atoms in the film. The
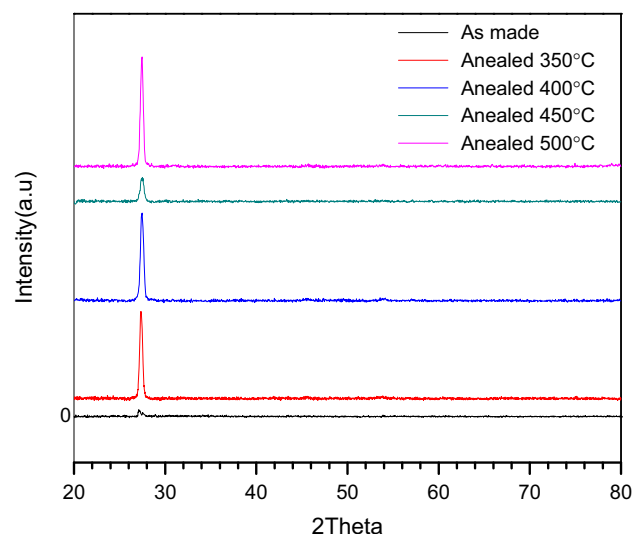

Fig. 1 XRD of ZnSe films annealed at different temperatures
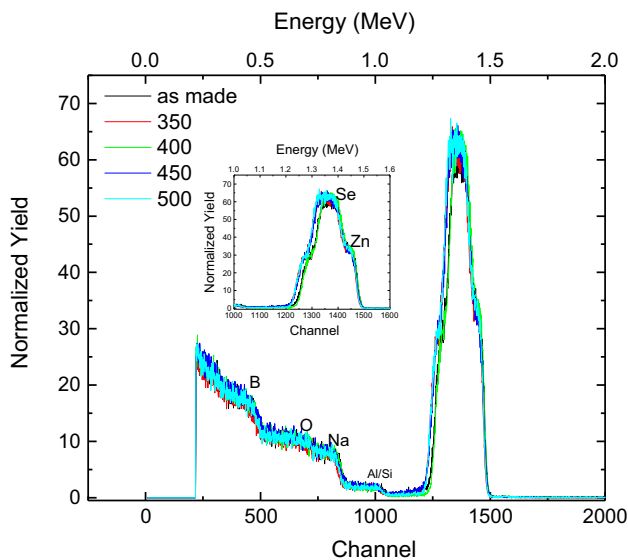
Fig. 2 Rutherford backscattering spectrum of ZnSe thin films annealed at different temperatures

composition and thickness of the films have been obtained through SIMNRA and RUMP simulation softwares. The thicknesses of the films used in these studies are given in Table 1. The RBS spectrum of ZnSe/glass thin film also shows that there is no interdiffusion of thin film and substrate material even after post deposition annealing.

The transmission spectroscopy of ZnSe/glass films was performed in the wavelength range of 300–1200 nm by optical spectrophotometer. ZnSe films have higher transmission between 400 and 700 nm showing that ZnSe is a suitable material for the window layer in thin film solar cells. The optical transmission of the films was found to increase with the increase of annealing temperature, Fig. 3. The increase in the transmission of the ZnSe thin films is probably associated with the oxygen reduction due to vacuum annealing. The removal of oxygen from the materials might have eliminated even trace amounts of $ZnO(SeO_2)$ present in the grain boundary regions, resulting in also the increase in crystallite size. The transmission spectra are used to calculate the absorption coefficient (α) with $\alpha = \frac{1}{d}\ln(1/T)$; T is transmission and d is the thickness of the sample. The band gap is calculated by drawing an intercept on the linear portion of $(\alpha h\nu)^2$ versus ($h\nu$) plot. The intercept at ($h\nu$) povides the band gap energy. It has been observed from these calculations that the band gap energies are increased from 2.45 to 2.54 eV with an increase in annealing temperature, Fig. 4 and Table 2.

Table 1 Thickness of ZnSe films with annealing temperature

Annealing temperature (°C)	As-made	350	400	450	500
Thickness (nm)	155	161	147	158	159
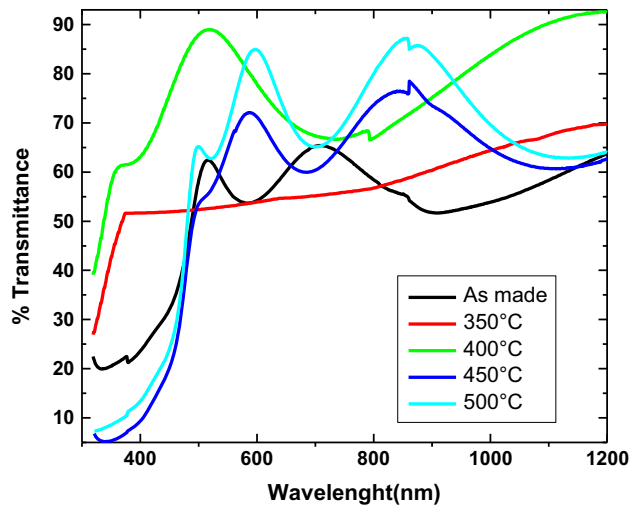
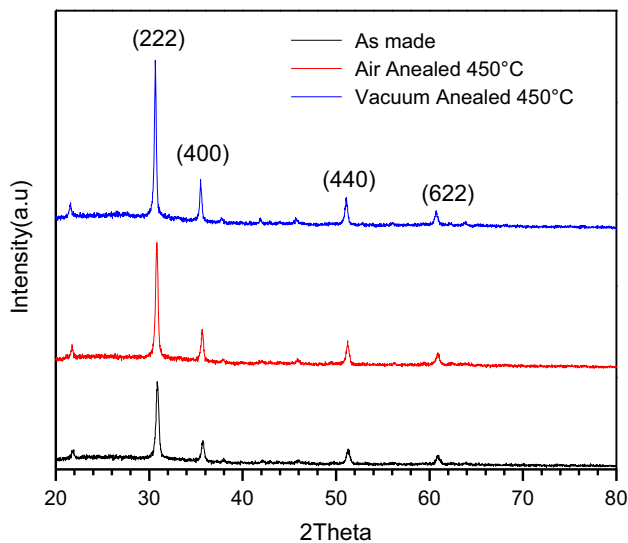Fig. 3 Transmittance spectra of ZnSe thin films at different annealing temperatures

The current–voltage characteristics (not shown) of ZnSe/glass thin films have shown that electrical conductivity is increased with the increase of post deposition temperature. The fabrication technique, annealing temperature, and doping profile control the grain growth of the films, therefore, the enhancement of conductivity with the increase of annealing temperature is most likely due to the increase in crystallite size, which is confirmed in the later discussion. The lowest value of the resistance is observed in the samples after annealing at 450 °C. Therefore, we synthesized ZnSe thin films on Indium Tin Oxide (ITO) substrate at 450 °C and annealed the samples in the air as well as in vacuum to correlate its structural and optical properties to the oxygen reduction from the sample. Since oxygen is one of the impurities that have the strongest
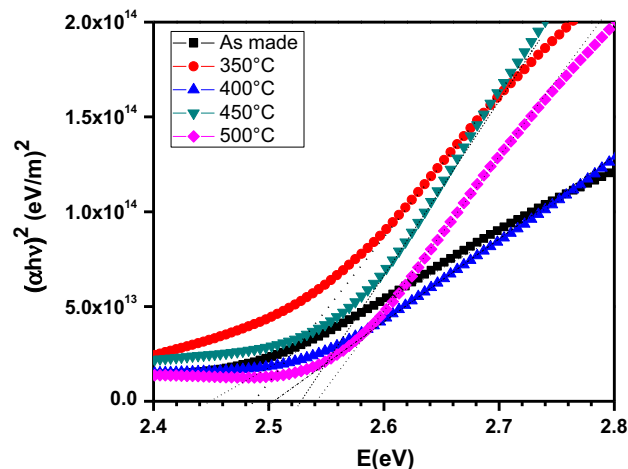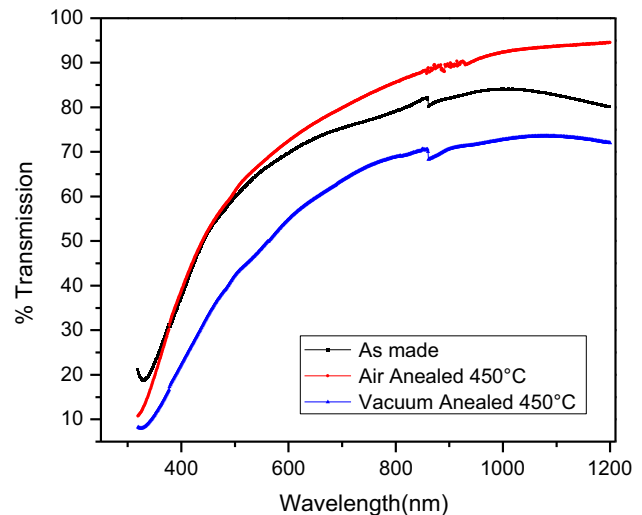

Fig. 4 Plot of $(\alpha h\nu)^2$ versus $h\nu$ of ZnSe thin films annealed at different temperature

Table 2 Band gap values of the ZnSe films on glass substrate after annealing in vacuum

Annealing temperature (°C)	Band gap (eV)
As-made	2.45
350	2.49
400	2.51
450	2.53
500	2.54

Fig. 6 Transmittance spectra of ZnSe/ITO thin films at different annealing temperatures

Fig. 5 X-ray diffractograms of ZnSe-ITO films annealed at various environments

effect on the structural and optical properties of zinc selenide, therefore, we have also performed post deposition annealing of ZnSe/ITO thin films at 450° in vacuum and air ambient to observe the effect of oxygen inclusion in the material on its structural and optical properties. Moreover, due to high reactivity of ZnSe, its contamination with oxygen during the preparation process is difficult to prevent [21]. The XRD spectra of ZnSe thin films on a ITO substrate (ZnSe/ITO) is shown in Fig. 5. These films have shown the zinc blend structure with a preferred orientation

along (222) plane at $2\theta = 30.85°$. The ZnSe thin films deposited on ITO substrate have shown higher band gap energy as compared to that of ZnSe deposited on glass substrate. Since the Fermi-level of ZnSe is higher than transparent conducting ITO there is a flow of the charge carriers from the ZnSe towards the ITO, therefore, it is suggested that due to the difference in the Fermi-levels of ITO and ZnSe more vacant states are created in the conduction band of ZnSe thereby promoting an increase in the energy gap.

The analysis of the XRD data have shown that the crystallinity of ZnSe/ITO/glass thin films has been improved after vacuum annealing and no shifts in peak positions were observed. The vacuum annealing was also resulted in the increase of crystallite size as discussed earlier in the discussion, whereas the strain and dislocation density have been decreased, Table 3. The transmission spectra of ZnSe/ITO/glass films taken from 300 to 1200 nm wavelength range are shown in the Fig. 6. It can be seen from this figure that transmission was increased with annealing at 450°C in air. The band gap values

Table 3 Structural parameters of the ZnSe-ITO films annealed in different ambient

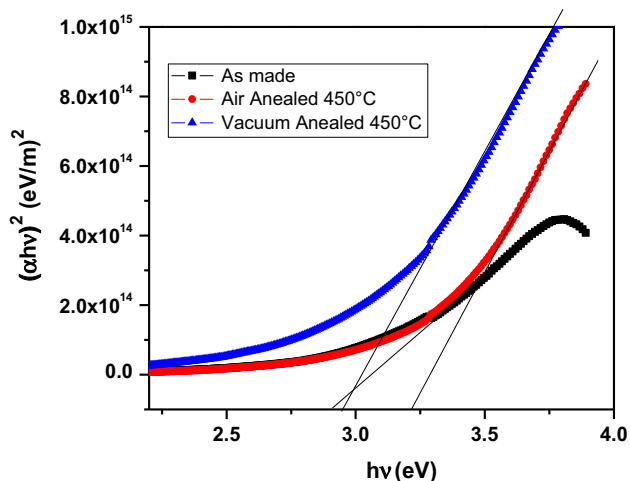| Material	Annealing	Temperature (°C)	2θ	d (Å)	a (Å)	(β)	Particle size (nm)	Strain (lines^2 m^{-4})	Dislocation density (line m^{-4})
ZnSe/ITO	As-made	As-made	30.85	2.89	10.01	0.410	20.31	17.24×10^{-4}	1.25×10^{15}
ZnSe/ITO	Vacuum	450°C	30.65	2.91	10.09	0.237	35.12	9.97×10^{-4}	0.42×10^{15}
ZnSe/ITO	Air	450°C	30.89	2.89	10.01	0.396	22.57	15.51×10^{-4}	1.01×10^{15}

Fig. 7 Plot of $(\alpha h\nu)^2$ versus $h\nu$ of ZnSe/ITO films

Table 4 Optical band gap of the ZnSe/ITO films annealed at 450°C

Annealing	Band gap
As prepared	2.90
Vacuum annealed	2.94
Air annealed	3.21

Fig. 8 I–V characteristics of ZnSe/ITO films

determined from $(\alpha h\nu)^2$ versus $(h\nu)$ plot (Fig. 7) are shown in Table 4. It can be seen that the increase in energy gap is highest in air annealed samples. It is most likely that during the deposition of the films at lower substrate temperature (close to room temperature) some states have been introduced vacancies and dislocations closer to the bottom of the conduction band and/or top of the valence band, which is resulted in the lowering of the energy gap. However, the post deposition annealing of the samples closer to the intercalation temperature of oxygen is resulted in the removal of impurity states from the sample. Due to the removal of oxygen from the material by annealing, the density of states introduced by inadvertent oxygen is reduced thereby promoting increase in the bandgap of ZnSe. On the other hand the increase in bandgap energy of vacuum annealed sample is smaller compared to that of air annealed ZnSe thin film is possibly due to the recrystallization of ZnSe in the absence of any source of oxygen intake from the atmosphere, which has been resulted in pure ZnSe thin film sample having energy gap close to ideal 2.7 eV. The inadvertent inclusion of oxygen in ZnSe most likely promotes the formation of oxides thereby also increasing the resistance of the samples. This was also confirmed in the IV-measurements of the samples, Fig. 8. In IV measurements the samples have shown Ohmic behavior and their resistance was decreased after vacuum annealing, which was otherwise increased after air annealing, Table 5. In vacuum annealing no oxygen is available and in turn no oxide formation takes place in the samples and consequently lower resistance in the samples is observed. These results of post deposition experiments suggest that by controlling the post deposition parameters such as annealing temperature and ambient the energy band gap of ZnSe can be easily controlled. More precise control over those parameters can help to achieve bang gap energy for required applications.

4 Conclusion

The experiments and preceding discussion have shown that the optical, structural and electrical properties of ZnSe thin films are sensitive to the post deposition treatment and the substrate material. The deposition of ZnSe thin films on a

Table 5 Electrical parameters of the ZnSe thin films on ITO annealed at 450°C

Material	Annealing	Temperature (°C)	Resistance $\times 10^3$ (Ω)	Sheet resistance $\times 10^3$ ($\Omega/\square$)
ZnSe-ITO	As-made	As-made	0.15	0.4
ZnSe-ITO	Vacuum	450	0.10	0.2
ZnSe-ITO	Air	450	0.17	0.5

substrate like Indium Tin Oxide is resulted in higher band gap energy as compared to that of the ZnSe deposited on a clean glass substrate. The difference in bandgap of ZnSe thin films on two different substrates is due to the fact that Fermi-level of ZnSe is higher than that of transparent conducting ITO, which is resulted in a flow of carriers from the ZnSe towards the ITO. This flow of carriers towards ITO causes the creation of more vacant states in the conduction band of ZnSe and increased the energy gap. Whereas, the post deposition treatment in vacuum and air ambient is resulted in the shift of optical band gap to higher side, however, the increase in the band gap energy is higher in the air annealed sample. It is therefore concluded that precisely controlling the post deposition parameters i.e. annealing temperature and the ambient the energy band gap of ZnSe can be easily tailored for desired properties.

References

1. T. Shirakawa, Mater. Sci. Eng. B **91**, 470 (2002)
2. E. Dynowska, M.M. Godlewski, E.M. Godys, M.R. Phillips, J. Lumin. **102**, 455 (2003)
3. W.-S. Lour, C.-C. Chang, Solid State Electron. **39**, 1295 (1996)
4. B. Ullrich, Mater. Sci. Eng., B **56**, 69 (1998)
5. L. Yan, J.A. Woollam, E. Franke, J. Vac. Sci. Technol., A **20**, 693 (2002)
6. H.R. Dobler, Appl. Opt. **28**, 2698 (1989)
7. Y. Noda, T. Ishikawa, M. Yamabe, Y. Hara, Appl. Surf. Sci. **113**, 28 (1997)
8. T.W. Kim, M. Jung, D.V. Lee, E. Oh, S.D. Lee, H.D. Jung, M.D. Kim, J.R. Kim, H.S. Park, J.Y. Lee, Thin Solid Films **298**, 187 (1997)
9. Q. Liu, H. Lakner, W. Taudt, M. Heuken, C. Mendorf, K. Heime, E. Kubalek, J. Cryst. Growth **197**, 507 (1999)
10. A. Pizzo, M.A. Tagliente, L. Caneve, S. Scaglione, Thin Solid Films **368**, 8 (2000)
11. M. El Sherif, F.S. Terra, S.A. Khodier, J. Mater. Sci.—Mater. Electron. **7**, 391 (1996)
12. R.F.C. Farrow, G.R. Jones, G.H. Williams, I.M. Young, Appl. Phys. Lett. **39**, 954 (1981)
13. S. VenKatachalam, S. Agilan, D. Mangalary Sa, K. Narayandass, Mater. Sci. Semicond. Process. **10**, 128 (2007)
14. E. Bacaksiz, S. Aksu, I. Polat, S. Yılmaz, M. Altunbas, J. Alloys Compd **487**, 280 (2009)
15. S. Venkatachalam, S. Agilan, D. Mangalaraj, S.K. Narayandass, Mater. Sci. Semicond. Process. **10**, 128 (2007)
16. Jeewan Sharma, Deep Shikha, S.K. Tripathi, Romanian Rep. Phys. **66**, 1002 (2014)
17. G.I. Rusu, V. Ciupina, M.E. Popa, G. Prodan, G.G. Rusu, C. Baban, J. Non-Cryst. Solids **352**, 1525 (2006)
18. Nicolae Spatalu, DormidontSserban and Tamara Potlog Spencer, N.D., J.H. Moore, Encyclopedia of Chemicla physics and Physical Chemistry: Fundamentals 2001: Institute of Physics Pub
19. K. Prabakar, S. Venkatachalam, Y.L. Jeyachandran, S.K. Narayandass, D. Mangalaraj, Sol. Energy Mater. Sol. Cells **81**, 1 (2004)
20. C.K. De, N.K. Mishra, Indian J. Phys. **71**, 530 (1997)
21. V.V. Blinov, E.M. Gavrishchuk, V.G. Galstyan, Inorg. Mater. **37**, 1228 (2001)